HHS Public Access

Author manuscript

Cell Rep. Author manuscript; available in PMC 2024 April 23.

Published in final edited form as:

Cell Rep. 2024 March 26; 43(3): 113861. doi:10.1016/j.celrep.2024.113861.

Identifying potential dietary treatments for inherited metabolic disorders using *Drosophila* nutrigenomics

Felipe Martelli[1,10], **Jiayi Lin**[1,10], **Sarah Mele**[1], **Wendy Imlach**[2], **Oguz Kanca**[3], **Christopher K. Barlow**[4], **Jefferson Paril**[5], **Ralf B. Schittenhelm**[4], **John Christodoulou**[6,7], **Hugo J. Bellen**[3], **Matthew D.W. Piper**[1,9,*], **Travis K. Johnson**[1,8,9,11,*]

[1]School of Biological Sciences, Monash University, Clayton, VIC 3800, Australia

[2]Department of Physiology, Monash Biomedicine Discovery Institute, Monash University, Clayton, VIC 3800, Australia

[3]Department of Molecular and Human Genetics and Duncan Neurological Research Institute at Texas Children's Hospital, Baylor College of Medicine, Houston, TX, USA

[4]Monash Proteomics & Metabolomics Facility, Monash Biomedicine Discovery Institute & Department of Biochemistry and Molecular Biology, Monash University, Clayton, VIC 3800, Australia

[5]School of BioSciences, The University of Melbourne, Melbourne, VIC 3052, Australia

[6]Murdoch Children's Research Institute, Parkville, VIC 3052, Australia

[7]Department of Paediatrics, The University of Melbourne, Melbourne, VIC 3052, Australia

[8]Department of Biochemistry and Chemistry and La Trobe Institute for Molecular Science, La Trobe University, Bundoora, VIC 3086, Australia

[9]Senior author

[10]These authors contributed equally

[11]Lead contact

SUMMARY

Inherited metabolic disorders are a group of genetic conditions that can cause severe neurological impairment and child mortality. Uniquely, these disorders respond to dietary treatment; however, this option remains largely unexplored because of low disorder prevalence and the lack of a

*Correspondence: matthew.piper@monash.edu (M.D.W.P.), t.johnson@latrobe.edu.au (T.K.J.).

AUTHOR CONTRIBUTIONS

Conceptualization, M.D.W.P. and T.K.J.; methodology, F.M., J.L., S.M., H.J.B., and O.K.; investigation, F.M., J.L., W.I., O.K., and C.K.B.; visualization and analysis, F.M., J.L., S.M., W.I., C.K.B., J.P., R.B.S., M.D.W.P., and T.K.J.; funding acquisition, H.J.B., O.K., M.D.W.P., and T.K.J.; project administration, M.D.W.P. and T.K.J.; supervision, J.C., M.D.W.P., and T.K.J.; writing, F.M., J.L., M.D.W.P., and T.K.J.

DECLARATION OF INTERESTS

The authors declare no competing interests.

SUPPLEMENTAL INFORMATION

Supplemental information can be found online at https://doi.org/10.1016/j.celrep.2024.113861.

suitable paradigm for testing diets. Here, we screened 35 *Drosophila* amino acid disorder models for disease-diet interactions and found 26 with diet-altered development and/or survival. Using a targeted multi-nutrient array, we examine the interaction in a model of isolated sulfite oxidase deficiency, an infant-lethal disorder. We show that dietary cysteine depletion normalizes their metabolic profile and rescues development, neurophysiology, behavior, and lifelong fly survival, thus providing a basis for further study into the pathogenic mechanisms involved in this disorder. Our work highlights the diet-sensitive nature of metabolic disorders and establishes *Drosophila* as a valuable tool for nutrigenomic studies for informing potential dietary therapies.

In brief

Martelli et al. use the fruit fly *Drosophila* to find dietary interventions for a large group of genetic disorders causing significant childhood mortality. They show that adjusting specific nutrients restores health and survival in a representative disorder. These findings may lead to targeted dietary therapies for patients.

Graphical abstract

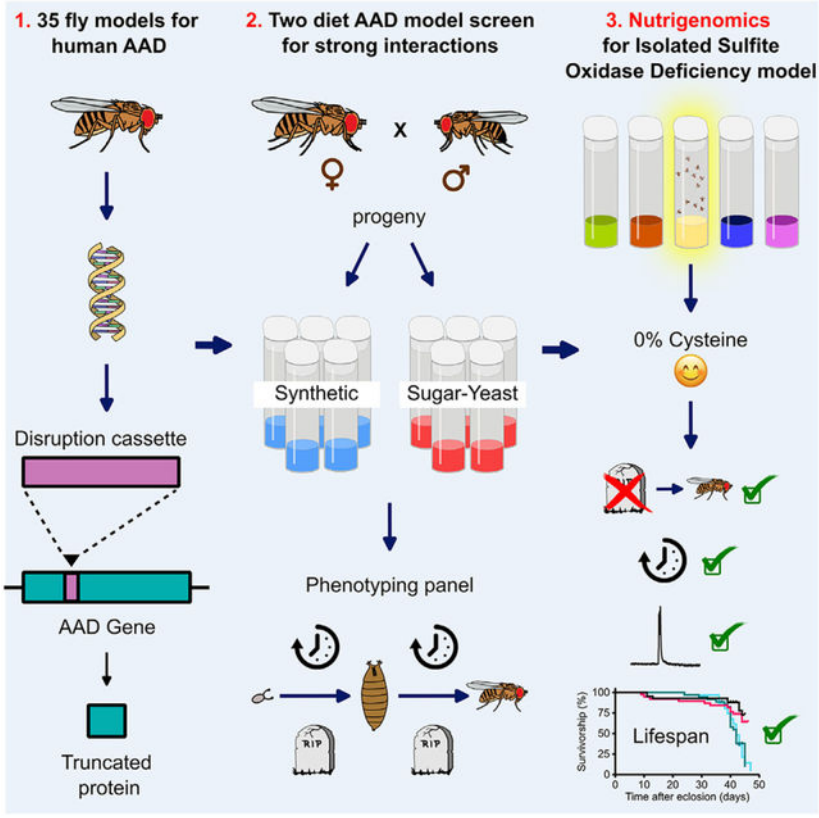

INTRODUCTION

Inherited metabolic disorders (IMDs) are a large and heterogeneous group of more than 1,000 rare genetic diseases with a global prevalence of 50.9 cases per 100,000 live births.[1,2] The largest class of IMDs is the amino acid disorders (AADs), which affect the metabolism

and transport of amino acids.[1] AADs commonly present with metabolic crises in infancy, with symptoms such as feeding difficulty, metabolic acidosis, hyperammonemia, and coma. If not detected and treated promptly, the most severe forms of AADs can lead to progressive neurodegeneration, motor deficits, and mortality shortly after birth.[1,3]

In contrast to most monogenic diseases, AADs are widely regarded as potentially treatable conditions.[4] This is because tissue metabolite levels, which are disrupted in AADs, are detectable and can be influenced by dietary manipulations.[5,6] Successful dietary treatment is illustrated by the most prevalent AAD, phenylketonuria, where implementation of a phenylalanine-restricted diet prevents newborns from neurodevelopmental complications.[7] However, close to 60% of AADs have no current effective treatment,[2] and as AADs are rare conditions, in most cases, systematic trials of any recommended dietary treatments are difficult to achieve. It therefore remains a significant challenge to reduce the pediatric morbidity and mortality associated with AADs.[1]

Laboratory animals have been utilized to model many metabolic diseases including AADs.[8–12] Mouse models have been the preferred system, partially due to close genetic and physiological traits with humans. For example, over 30 mouse models have been created and used to dissect AAD mechanisms.[13] Very few of these studies, however, have focused on evaluating dietary treatments because of the cost and time associated with complex large-scale feeding trials with mice and the challenges associated with manufacturing nutrient-varied semi-synthetic diets.

An animal well suited to study nutrigenetic interactions in disease models is the fruit fly *Drosophila melanogaster*.[13] In addition to their genetic tractability, a key benefit is that *Drosophila* can be reared quickly, permitting large cohorts of genetically similar individuals to be surveyed across an array of different conditions at a relatively low cost.[14] These features, coupled with the recent development of a defined fully synthetic diet that allows for the complete manipulation of its composition,[15] enable exploration of genotype-nutrient interactions at high resolution.

Drosophila have been previously used to study AADs, owing to the extensive conservation between flies and humans in the uptake, transport, metabolism, and usage of amino acids.[13] For example, fly models for maple syrup urine diseases[16] and hyperprolinemia type I[17] and type II[18] have been used to investigate the molecular basis and the pathogenic mechanisms of these disorders. Flies harboring a mutation in the delta-1-pyrroline-5-carboxylate dehydrogenase (*P5CDh*) gene were the first to correlate loss of *P5CDh* function, mitochondrial defects, increased levels of proline, and intellectual disability in hyperprolinemia type II.[18] Similar valuable insights have been gained with a model of isolated sulfite oxidase deficiency (ISOD), which recapitulates the high levels of sulfite seen in patients, revealing that larval locomotor deficits were the result of a metabolic dysregulation in ensheathing glial cells.[9]

Despite these advantages, *Drosophila* has not been used to systematically explore dietary compositions that may be beneficial for patients with metabolic diseases. Here, we describe a low-cost nutrigenomic pipeline for revealing disease-nutrient interactions of potential

clinical value using *Drosophila*, focusing on the treatment of AADs. We generated a catalog of 35 fly AAD models and assessed their survival and developmental progression raised on both a standard sugar-yeast (SY) diet and a synthetic diet.[15] Our data describe strong loss-of-function phenotypes for our models and reveal that many are diet sensitive, suggesting that therapy may be possible through precision nutrition. We used a multi-nutrient array to dissect the nutritional basis of the diet response for a model of ISOD, a severe AAD affecting sulfur amino acid metabolism. These experiments identified nutrient compositions that restored physiology and metabolic profiles close to the control state, thus pointing to a potential new dietary therapy for this disorder. Our work establishes *Drosophila* as an animal model for disease nutrigenomics, with the goal of expanding the treatment options available to patients.

RESULTS

A screen for diet-responsive AADs in *Drosophila*

The *Drosophila* genome contains single highly conserved orthologs for 81 of the 114 AAD-causing human genes currently known.[13] We prioritized these based on human AAD severity, excluding those commonly reported as benign, and created a catalog of loss-of-function mutant lines representing 35 *Drosophila* AAD models (Tables 1 and S1A). For genetic background consistency, the majority of these models (32/35) were generated using a Minos-mediated cassette exchange system or its CRISPR-mediated revision[19–22] to disrupt endogenous gene expression and instead express the yeast transcription factor GAL4 (Table S1A). Alleles for the remaining three genes were made via CRISPR-Cas9 mutagenesis, with one sourced from a previous study.[9]

To reveal fly AAD models with phenotypes modifiable by diet, we devised a two-diet screen using both a standard SY fly medium and a recently devised synthetic complete medium that fully supports the preadult period[15,56] (Figure 1A). The SY medium is widely used in *Drosophila* research and is based on natural ingredients, sugar, and yeast (Table S2). In contrast, the synthetic medium is chemically defined, allowing for manipulation of individual nutrients, including each of the 20 proteinogenic amino acids (Table S2). Based on the nature of the generated alleles and the AADs they represent, we expected that many would be lethal when homozygous or would show developmental delays, and therefore we used these traits to look for diet-genotype interactions. When raised on the SY diet, 33/35 (94%) AAD models showed a significant developmental delay in comparison to their respective controls (heterozygous animals [AAD/+], or +/+ [w^{1118} strain] if X-linked), and 24/35 (68%) significantly impacted survival, including 11 that were lethal, with 6 arresting at prepupal stages (Table S1B). On the synthetic diet, 29/35 (83%) AAD models were significantly delayed in development relative to controls, and 27/35 (80%) showed reduced survival, including 12 that were lethal (Table S1B). Together, all of the AAD models we tested showed a significant impairment in at least one of the four traits tested.

Comparing across the two diets revealed striking phenotypic differences among the AAD models. For developmental delay, 21/35 (60%) of the AAD models showed a significant response to diet (Figures S1 and S2; Table S1B). For survival, 12/35 (34%) of the AAD fly models were significantly affected by diet (Figures S1 and S2),

with 9 of these impacting egg-to-adult viability, causing at least a 20% difference in mean adult survivorship between dietary conditions (Figures 1B and 1C; Table S1B). Overall, significant diet interactions were observed for 25/35 (71%) of the AAD models (Figures 1C, S1, and S2). Notably, 3 AAD models showed significant diet-genotype interactions for all of the four traits measured: *CG15093* (human ortholog HIBADH-3-hydroxyisobutyrate dehydrogenase deficiency), *shop* (human ortholog SUOX-isolated sulfite oxidase deficiency), and *Argl* (human ortholog ASL-argininosuccinate lyase deficiency) (Figure 1C; Table S1A). *CG15093* and *shop* diet responses were most striking, showing normal survival on SY medium and near or complete lethality on the synthetic diet (Figure 1B). Given that the 25 diet-responsive AAD models cover many critical and distinct metabolic pathways (e.g., branched-chain amino acids, cysteine and methionine, and the urea cycle), our results suggest that the diet-metabolism interaction may be widely exploitable for diet-based therapy.

Nutrient-disease interactions revealed by nutrigenomic analysis in a *Drosophila* ISOD model

By using the synthetic diet for our initial screen, we had an opportunity to explore the nutritional bases of the diet-responsive fly AAD models. As a proof of concept, we chose to focus on *shop*, as it represents a previously validated model of ISOD.[9] In its classic form, ISOD is a severe condition that causes seizures, feeding difficulties, progressive microcephaly, and intellectual disability, with patients usually dying within the first year of life.[57] ISOD is caused by the accumulation of neurotoxic metabolites including sulfite, thiosulfate, and S-sulfocysteine resulting from failure at the final step in catabolism of the sulfur-containing amino acids (methionine and cysteine)[58,59] (Figure 2A). Methionine (Met) is an essential dietary nutrient and precursor for cysteine (Cys) biosynthesis, with input from the non-essential amino acid serine (Ser) (Figure 2A).

In order to understand whether manipulation of these three dietary amino acids could restore health to the ISOD flies, we tested an array of 75 diets comprising their three-way dose-responses (5 [Cys] × 5 [Ser] × 3 [Met] doses; Figure 2B; Table S1C). We found that depleting Met, Ser, and Cys individually or in combination rescued the lethality of the *shop* mutation to varying extents, resulting in viable adults (Figure 2B; Table S1C). Interestingly, we detected significant interactions between all three amino acids, and also between Ser and Cys, indicating that these nutrients have synergistic effects on the ISOD model disease state (Table S1D). These diet effects were specific for sulfur-containing amino acids, as depletion of other amino acids such as phenylalanine and tyrosine yielded no benefit to ISOD flies (Figure S4). Cys depletion had the largest single-nutrient effect, with normal adult survival observed when Cys alone was depleted (Figure 2C; Table S1C). The developmental timing of *shop* mutants reared on 0% Cys was also rescued, and notably, the timing of control flies was unaffected by the Cys-free diet (Figure 2D). By transferring *shop* individuals at intervals during the larval stage from the complete to the Cys-free media, we further narrowed the critical treatment window for full adult survivorship to the first 6 days of larvalhood (Figure 2E). Thus, larval Cys restriction is necessary and sufficient to restore viability in *shop* mutants. Given this remarkable restoration of development and viability, we used the 0% Cys diet for subsequent experiments.

Metabolic basis of *Drosophila* ISOD dietary rescue

Having established the importance of the Cys-free diet to the ISOD model larvae, we were in a position to ask how the diet shifts *shop* metabolism during this stage. For this, we performed untargeted metabolomics on 5-day-old *shop* and control larvae raised on either 100% or 0% Cys. Principal-component analysis on the 1,381 putatively identified metabolites (Table S1E) distinguished the ISOD disease state from controls on the same diet (Figure 3A). Remarkably, *shop* mutants reared on 0% Cys had restored metabolite levels, grouping tightly among the control samples that were raised on the same diet and notably separated from the ISOD disease state. Indeed, the largest responses across the 921 significantly affected metabolites (ANOVA $p < 0.05$) were those in the *shop* mutant samples between the diets (Figures 3B and S4; Table S1E). An enrichment analysis on *shop* larvae reared on 0% Cys in comparison to 100% Cys revealed a reduction in pathways related to urea cycle and ammonia recycling, and an increase in energy pathways such as fatty acid biosynthesis and β-oxidation, potentially indicating a general restoration of energy homeostasis (Figure S5). As might be expected, control larvae on the 0% Cys diet showed general reductions in Cys metabolism and related pathways (e.g., taurine) and modest elevations in central energy generation (e.g., citric acid cycle; Figure S5).

Among the metabolites that differed in the *shop* larvae between diets, we found strong reductions in neurotoxic metabolites that are also markers of the disease in patients such as thiosulfate and S-sulfocysteine[60] (Figure 3B). High levels of glutathione-sulfite were detected in mutants raised on a 100% Cys diet, suggesting an effort to sequester excess sulfite for detoxification[61] (Figure 3B). Additionally, we detected elevated sulfonic acid, a byproduct of sulfite oxidation,[62] in *shop* reared on 100% Cys, levels of which were also significantly reduced by the Cys-free diet (Figure 3B). To test the contribution of these metabolites to the *shop* phenotype, we performed supplementation trials. Adding sulfite (the substrate of sulfite oxidase) or thiosulfate to the Cys-free diet significantly reduced the health of *shop* larvae (and not controls), suggesting they play a causative role in *Drosophila* ISOD pathogenesis, consistent with mammalian model data and cell culture studies[63,64] (Figures 3C and 3D). Adding N-acetylcysteine (NAC) in order to support intracellular glutathione replenishment did not rescue the *shop* phenotype; however, because NAC itself is a source of Cys, we cannot rule out that glutathione is protective in the disease state (Figure S6).

Looking more broadly at the sulfur-amino acid pathway metabolites we detected, we found that the 0% Cys diet had a strong effect on metabolites downstream of Cys, irrespective of genotype (Figure 3E). Notably, cystathionine, the immediate precursor for Cys biosynthesis, was elevated in *shop* larvae reared on 100% Cys, as was 3-sulfinoalanine, the product of Cys oxidation, and both were normalized by the 0% Cys diet (Figure 3E). Sulfate (the product of sulfite oxidase) was not significantly reduced in *shop* mutants (Figure 3E), possibly because there are alternative sources of sulfate (e.g., sulfatase activity[65] or gut microbiota[66]). The striking reduction in apparent pathway flux on the 0% Cys diet made us curious about its transcriptional regulation. Surveying the transcript levels of several critical pathway gene products acting up- and downstream of Cys, we found strong downregulation in larvae on the Cys-free diet, possibly as a response to prevent catabolism of Cys when restricted

in the diet (Figure S7). Genes dysregulated in *shop* larvae on 100% Cys diet (*Eip55E* [*CTH*], *Sam-s* [MatI-III], and *Sqor* [*SQOR*]) were largely normalized by the Cys-free diet, suggesting that not only is this treatment highly effective at restoring metabolic cellular homeostasis but it also restores transcriptional regulation.

Enrichment analysis of the metabolomics data suggested that central energy metabolism was also impacted by the Cys-free diet (Figure S5). Indeed, we found that the key metabolites alanine, pyruvate, and lactate, which were elevated in the *shop* larvae, were fully restored when reared on the Cys-free diet (Figure 3F). Consistent with this, cellular energy impairments indicated by imbalanced proportions of NADH/NAD and ATP/ADP + AMP, suggestive of increased demand to recover cytoplasmic NAD+ for glycolysis, were also largely normalized (Figure 3F). These restored metabolite levels observed in *shop* mutants support the ability of Cys depletion to effectively address the metabolic crisis. We queried whether oxidative stress could be a cause of impaired energy metabolism by looking for transcriptional changes in a suite of oxidative-stress-related genes (e.g., *Nrf2* and *SOD*). We found only very mild upregulation of nitric oxide synthase in *shop* mutants reared on Cys-free diet, implying either a localized disruption beyond our detection or that reactive oxygen species is not a major contributor to pathogenesis (Figure S7).

Drosophila ISOD larval behavior, physiology, and adult longevity are restored by feeding larvae a Cys-free diet

The profound metabolic correction detected in *shop* mutants on the Cys-free diet likely explains the broad phenotypic health improvements we observed. However, given that disease markers were still mildly elevated compared to controls (Figure 3B), we remained unsure whether function at the tissue level, including neurophysiology, was similarly restored. *shop* mutant larvae were initially reported to have behavioral defects caused by impaired neurotransmission.[9] We therefore asked whether these neurological issues were also restored by Cys depletion. We found that locomotor behavior of *shop*, measured on 5-day-old larvae (prior to any signs of larval arrest), was restored to the control level by Cys depletion, which is consistent with the improvement observed for other traits (Figure 4A).

For a direct and more sensitive readout of neurotransmission, we performed electrophysiological recordings from the neuromuscular junctions of these larvae (second instar). Upon stimulation, we observed a strong reduction in excitatory junction potential (EJP) amplitudes for *shop* mutant larvae, suggesting marked neurotransmission impairment (Figure 4B), which is consistent with a previous report.[9] However, this returned to normal levels in individuals raised on the Cys-free diet (Figure 4B). Similarly, spontaneous synaptic events (miniature EJP) were near absent in *shop* mutant larvae and returned to a normal frequency by the Cys-free diet (Figure 4C), suggesting that the diet rectifies a major impairment in presynaptic neurotransmitter release.[67]

Finally, since the diet rescued *shop* larvae to adulthood, we sought to assess health of the rescued *shop* adults and determine if continued Cys depletion was needed to avoid disease. For this, we tracked the longevity of *shop* mutant flies raised on 0% Cys food during larval stages and transferred to complete or 0% Cys food as adults. *Shop* adults raised on 0% Cys during larval stages have a slightly reduced adult lifespan; however, this effect was

unaltered by the Cys content of adult food, suggesting that Cys restriction in the larval diet is necessary and sufficient for lifelong *shop* health (Figure 4D). Interestingly, thiosulfate levels at 7 and 14 days of adulthood remained consistent and did not differ from controls, suggesting that Cys metabolism in ISOD adult flies can cope when fed a Cys-containing diet (Figures 4E and S8). Taken together, these data demonstrate that removal of a single non-essential dietary nutrient largely corrects the pathogenic metabolic profiles caused by ISOD, which, in turn, dramatically improves neurological function and lifelong health.

DISCUSSION

Around 60% of AADs currently have no known effective treatment, while many more could potentially benefit from optimizing existing dietary therapies.[2] However, the conventional method for exploring novel dietary therapies occurs in a clinical setting, where treatment decisions are typically made for single or few patients at a time. This means that progress remains slow, and causality between treatment and outcome can be challenging to assign. To address these obstacles, we sought to establish a complementary paradigm in which high-throughput nutrigenomics could be applied in an animal model to uncover diet-disease interactions that may be of direct clinical value to inform treatment attempts. For this, we selected *Drosophila melanogaster* because of its genetic tractability, strong conservation in metabolic systems with humans, and the availability of a customizable synthetic diet.

Within the set of 35 *Drosophila* models of human AADs we generated, we observed excellent concordance in terms of phenotypic severity compared to human disease data. AADs caused by loss of *SUOX, DBT, GLS, PHGDH, SHMT2*, and *ECHS1*, for example, are all severe conditions associated with poor clinical outcomes (Table 1) and similarly resulted in complete lethality in our fly models. Most strikingly, however, was that 25 of the 35 models were affected differently by the diet they were raised on, including two models (*shop* and *CG15093*) where diet determined life or death. Since our models represent diseases associated with all known amino acid metabolic pathways, these findings imply that the AAD phenotype is intimately linked to the nutritional environment. Importantly, this provides support to the idea that dietary interventions may be widely exploitable for therapeutic purposes.[68] Indeed, it has been known for 70 years that AADs such as phenylketonuria can be treated solely and effectively by dietary modification.[69,70] However, for many, AAD dietary intervention is ineffective and/or involves a general, non-specific, reduction in protein intake.[71] Thus, identifying disease-specific nutrient interactions could inform a new generation of tailored dietary compositions for clinical use.

Toward this end, we implemented a multi-nutrient diet array for the fly ISOD model targeting only dietary nutrients relevant to the sulfur-containing amino acid catabolic pathway (Met, Cys, Ser). Although co-restriction of Met and Cys has been identified as an effective treatment for late-onset ISOD,[72,73] our data suggest that Ser and Cys co-restriction, or Cys restriction alone, may be an effective and possibly safer alternative by avoiding restriction of the essential amino acid Met, which may cause harm (e.g., progressive sarcopenia and frailty[74,75]). While the more severe classic ISOD is currently considered untreatable, our data suggest that the pathway is highly responsive to Cys restriction, which warrants efforts to introduce treatment diets early or maternally.

Remarkably, the health restoration observed in the fly ISOD model in response to dietary Cys depletion was apparent at all levels of physiology. This demonstrates that simple dietary changes, such as altering the availability of a single micronutrient, can profoundly alter animal metabolism. Given that we detected strong diet-phenotype interactions for many of our models, we reason that this is likely to be the case for many other diseases. Understanding how this occurs will provide important new insights into disease pathogenesis, including the extent to which endogenous control mechanisms can keep disease at bay as well as the triggers for its onset and progression. Using diet-switching and dose-response experiments as we described here may allow more fine-scale control of disease onset and progression. These approaches coupled with resupplementation of potentially causative metabolites could yield important clues to the mechanisms of pathogenesis.

IMDs are a significant cause of childhood morbidity and mortality worldwide. However, their detectability and unique responsiveness to dietary modifications provide hope that advancements in nutrition may lead to better health outcomes for sufferers. Here, we show that *Drosophila* can be rapidly applied as both a scalable metabolic disease model and a nutrigenomic tool to explore diet-disease interactions. The pipeline we describe can be further applied to other diseases modeled in *Drosophila* where nutritional interactions may play a significant role in pathogenesis (e.g., cancer,[76] neurodegeneration[77]).

Limitations of the study

Differences in physiology between model organisms and humans may lead to varying responses to dietary changes. For example, unlike humans, *D. melanogaster* must obtain arginine from their diet due to insufficient production through the urea cycle. Consequently, modeling disorders related to arginine metabolism and the urea cycle may result in different phenotypic responses compared to humans. Another limitation arises from using null alleles to model these disorders, which may not accurately reflect the typical presentation seen in humans. This could affect the responsiveness of the models to diet and might explain why fly phenotypes tend to be more severe than those observed in human patients. Additionally, in our experiments, flies are confined to their diets from embryo to adulthood, lacking the dietary diversity experienced by humans. These limitations underscore the importance of validating findings in vertebrate models, such as mice or other rodents.

STAR★METHODS

RESOURCE AVAILABILITY

Lead contact—Further information and requests for resources and reagents should be directed to and will be fulfilled by the lead contact, Travis K. Johnson (t.johnson@latrobe.edu.au).

Materials availability—All unique/stable reagents generated in this study are available from the lead contact without restriction.

Data and code availability

- Metabolomics data have been deposited online at MetaboLIGHT and are publicly available as of the date of publication. The dataset identifier is listed in the key resources table.
- This paper does not report original code.
- Any additional information required to reanalyze the data reported in this work is available from the lead contact upon request.

EXPERIMENTAL MODEL AND STUDY PARTICIPANT DETAILS

All stocks of *Drosophila melanogaster* were maintained at 18°C on sugar-yeast medium under natural photoperiod conditions, and for experiments flies were reared in incubators at 25°C and 45% humidity on specific diets as described below.

METHOD DETAILS

Drosophila* AAD allele generation—Drosophila* lines listed in the key resources table without a 'Source' entry were generated for this study. Of these, MiMIC (MI) and CRiMIC (CR) alleles designated 'TG4' were converted to T2A-GAL4 containing alleles via Recombinase Mediated Cassette Exchange (RMCE) as previously described.[78] Correctly oriented and framed RMCE events were confirmed via UAS-YFP expression.[85,86] Alleles designated 'KO-kG4' (Kozak-GAL4) were generated as previously described.[22] The sgRNA and homology arm sequences and PCR verification details for each line can be found at https://flypush.research.bcm.edu/pscreen/crimic/crimic.php. For CRISPR/Cas9-induced point mutations, we crossed transgenically-expressed guide RNA lines targeting *Hn* and *Hmgcl* coding sequences to a maternal germline Cas9 source and isolated stable mutant lines bearing early frameshift mutations. All mutant lines used were first outcrossed to w^{1118} for removal of y^{1} and then maintained over fluorescently marked balancer chromosomes.

Diet preparation—Chemically defined media used in this study were prepared as described in Piper et al.,[15] with modifications to support larval development. Briefly, sucrose, agar, low solubility amino acids (L-isoleucine, L-leucine, and L-tyrosine), and stock solutions of buffer, metal ions and cholesterol were combined with MilliQ water using a magnetic stirrer. After autoclaving at 120°C for 15 min, the solution was cooled at room temperature with stirring to ~65°C. Stock solutions for amino acids, vitamins, nucleosides, choline, inositol, and preservatives were then added. Liquid food was dispensed into sterile vials. The chemically defined diet recipes, including modifications used for targeted nutrigenomics and dose-response assays, as well as the standard sugar-yeast medium are listed in the supplemental information (Table S2).

Larva collection and sorting—To obtain large numbers of developmentally synchronized first instar larvae, embryos were collected from population cages containing approximately 200 females and 50 males (5–10 days old) that were allowed to lay for 6 h on apple juice agar plates supplemented with yeast paste. Embryos were collected and washed with distilled water and then transferred to a new plate (yeast paste-free) and incubated at 25°C for 24 h to hatch. Homozygous individuals (AAD/AAD) were collected from cages

comprising heterozygous adults (the allele of interest and a fluorescently marked balancer chromosome). To collect AAD/+ individuals (controls), cages comprised heterozygous males and virgin w^{1118} (+/+) females. Where the gene of interest was X-linked, w^{1118} were used as a control.

First instar larvae were selected based on the absence of the fluorescent balancer. Using a blunt metal probe, larvae were transferred to the required medium. For the larval diet-switching experiment, larval locomotor assay, electrophysiology and metabolomic analysis, larvae at the desired developmental stage were collected by floating in 20% sucrose solution.[87] Briefly, 20% w/v sucrose solution was poured into each vial. The top layer of food was then gently disrupted with a metal probe in order to release the larvae. The solution with floating larvae was poured through a fine cloth mesh to isolate the larvae. Larvae were then rinsed three times with Phosphate Buffer Saline (PBS) and transferred to fresh media or microtubes tubes using a fine paintbrush.

Developmental timing and viability—Twenty first instar larvae were transferred to a vial containing the appropriate diet and monitored every 12 h for 25 days for the presence of pupae and adults. This was replicated 5 times per genotype per diet. The same approach was used to assess *shop* mutants and controls raised on modified synthetic media with 0% cysteine, 0% tyrosine, 50% phenylalanine and 75% phenylalanine.

Targeted multi-nutrient array—Large numbers of developmentally synchronized embryos obtained from multiple cages containing *shop*/FM7a,sChFP females were collected and washed in distilled water, and transferred to 15 mL tubes containing PBS. Once the embryos had settled (1 min), excess PBS was removed. Using a micropipette set to 5 μL and a tip cut to widen the bore, small volumes of embryos were aspirated and then dispensed into vials onto the medium surface. This was performed for each of the 75 modified synthetic diets tested with varied levels of cysteine, serine, and methionine replicated 5 times (Table S1B). Vials were checked daily for 20 days and the total number of adult flies were counted with the survival proportion of *shop* (*shop*/total flies) calculated. The total number of adults per vial ranged from 10 to 80 individuals (mean = 44.17, s.d. = 9.40).

Longevity—Larvae were reared on the 0% cysteine diet under constant density (20 per vial with 5 vials for *shop* and 10 vials for controls) and adult eclosion monitored daily. Adults of the same genotype that eclosed on the same day were combined and transferred evenly to either the 100% diet or 0% cysteine diet. Since *shop* is X-linked and *shop* hemizygous males are sterile,[9] only male flies (*shop* and control) were included in the longevity experiment. Flies were given fresh media and scored for survival three days per week. Escapees were censored from the analysis. Eight vials each containing 1 to 9 flies were tracked for *shop* per diet. Six vials each containing 1 to 14 flies were tracked for the control per diet.

Diet switching assay—Embryos were collected and dispensed on to the complete synthetic diet (100% cysteine) as per the multi-nutrient array. On days 2, 4, 6, and 8 post-hatching, larvae from 10 replicate vials were floated in 20% sucrose, washed, and transferred to fresh vials containing the 0% cysteine diet. An additional group of 10 vials were kept on the complete media as a control. Numbers of adult *shop* males and control

(FM7a, sChFP) males were scored for 20 days post egg-lay. The total number of adults per replicate ranged from 29 to 97 individuals (mean = 56.8, s.d. = 15.9).

Metabolic profiling—Five replicates of 10 five-day-old larvae from each genotype and diet condition were collected, washed in PBS, blotted dried, and weighed. Samples were then transferred to 1.5 mL safe lock microtubes tubes (Eppendorf), flash frozen in liquid nitrogen, and stored at −80°C. Thawed larvae were homogenized using a disposable pestle in 20 μL of ice-cold extraction solvent consisting of 2:6:1 chloroform:methanol:water with 2 μM of (CHAPS, CAPS, PIPES and TRIS) acting as internal standards. Once ground additional solvent was added to a final ratio of 20 μL of extraction solvent per mg of larvae. Samples were vortexed for 30 s and then sonicated in an ice-water bath for 10 min and centrifuged at 4°C (22,000 ×g for 10 min). The supernatant was then transferred to a glass vial for LC-MS based metabolomic analysis. 20 μL of each extract were combined to make a pooled quality control sample.

LC-MS was performed using a Dionex Ultimate 3000 UHPLC coupled to an QExactive Plus mass spectrometer (Thermo Scientific). Samples were analyzed by hydrophilic interaction liquid chromatography (HILIC) following a previously published method.[88] The chromatography utilized a ZIC-p(HILIC) column 5μm 150 × 4.6 mm with a 20 × 2.1 mm ZIC-pHILIC guard column (both Merck Millipore, Australia) (25°C). A gradient elution of 20 mM ammonium carbonate (A) and acetonitrile (B) (linear gradient time-%B: 0 min-80%, 15 min-50%, 18 min-5%, 21 min-5%, 24 min-80%, 32 min-80%) was utilized. Flow rate was maintained at 300 μL/min. Samples were stored in the autosampler (6°C) and 10 μL was injected for analysis. MS was performed at 70,000 resolution operating in rapid switching positive (4 kV) and negative (−3.5 kV) mode electrospray ionization (capillary temperature 300°C; sheath gas flow rate 50; auxiliary gas flow rate 20; sweep gas 2; probe temp 120°C). Samples were randomized and processed in a single batch with intermittent analysis of pooled quality-control samples to ensure reproducibility and minimize variation. For accurate metabolite identification, a standard library of ~500 metabolites were analyzed before sample testing and accurate retention time for each standard was recorded. This standard library also forms the basis of a retention time prediction model used to provide putative identification of metabolites not contained within the standard library.[89]

Larval locomotor assay—Locomotor assay modified from Brooks et al.[90] Five replicates of 5-day-old larvae for each genotype and diet condition were collected, washed in PBS and blotted dry then transferred using a blunt metal probe to a Petri dish containing SY medium with blue food dye (Queen) and allowed to acclimate for 3 min. The plate was placed on a uniform black background to reduce aberrant reflections and filmed for 3 min with a webcam (Logitech). The movie file was converted into avi format (ffmpeg), and analyzed in ImageJ using the wrMTrck plugin[91] (Table S1F). For each larva, the total length of movement (mm) was calculated. For each genotype and diet, 5 replicate plates (25 individuals total) were tracked.

Thiosulfate determination assay—Thiosulfate determination assay was modified from.[92] Five replicates of 20 7-day-old and 14-day-old adult flies, or 50 5-day-old larvae for each genotype and diet condition were collected and transferred to 1.7mL microtubes

(Eppendorf), frozen with liquid nitrogen. Thawed flies were homogenized to powder using a disposable pestle in 0.05% tween 20. Samples were then homogenized by vortexing for 20 s followed by centrifuging at 5000rpm for 1 min. For each sample, 500 μL supernatant was transferred individually to a new 1.7mL Eppendorf tube and centrifuged for 3 min at 14000rpm. For final data normalization, protein concentration of each sample was measured using Pierce BCA protein assay kit #23227. For thiosulfate determination, 250 μL supernatant from each sample was transferred individually to new 1.7mL Eppendorf tubes, followed by adding 750 μL methylene blue solution (a stock solution was prepared by dissolving 3 mg methylene blue in 250 mL 5M HCl). Samples were incubated at room temperature for 30 min. A standard curve based on a 1 mM freshly prepared sodium thiosulfate solution was prepared by transferring 0, 1, 5, 10, 20, 50, 75 and 100 μL sodium thiosulfate solution (these values correspond to the same amount of thiosulfate in nM) to fresh 1.7mL Eppendorf tubes. The volume was made up to 250 μL with 0.05% tween 20, followed by adding 750 μL methylene blue solution and incubated at room temperature for 30 min. For each experimental samples as well as the standard curve, 100 μL of solution was transferred to a 96-well plate (triplicates were prepared for experimental samples). Absorption at 670 nm was determined spectrophotometrically against 0.05% tween 20 as the reference.

Electrophysiology—Twenty-five 6-day-old larvae for each genotype and diet condition were collected, washed in PBS and blotted dry. Samples were then and transferred to 1.7mL microtubes (Eppendorf) containing 50μL PBS. Larvae were dissected and intracellular membrane potentials were recorded as previously described.[93] Briefly, recordings were performed on muscle 6 in segment A3. The free segmental nerve end was drawn into a microelectrode using an injector and stimulated with a DS2A isolated voltage stimulator (Digitimer) at 0.1 Hz with a suprathreshold stimulating pulse and postsynaptic potentials were recorded with electrodes (20–50 MΩ) filled with 3 M KCl. All recordings were conducted at room temperature with a Multiclamp 700B amplifier (Molecular Devices, Sunnyvale, CA) in current clamp using AxoGraph X software v1.7.6 (AxoGraph, Australia). A minimum of 20 EJPs were recorded per muscle and the average amplitude used. The mEJP recordings were done over a 2-min period and events detected by analyzed by fitting to a template in AxoGraph X.

RNA extraction and gene expression analysis by Real-Time qPCR—Three to five replicates of 40 five-day-old larvae from each genotype and diet condition were collected into microtubes containing 500 μL of TRIzol (Invitrogen). Total RNA was isolated on the same day following the manufacturer's instructions. RNA purity and concentration were evaluated by spectrophotometry (NanoDrop ND-1000, NanoDrop Technologies). RNA samples were then diluted to 5 μg/μL and stored at −80°C. RNA samples were treated with the RQ1 RNase-Free DNase (Promega) following the manufacturer's instructions to remove genomic DNA contamination and cDNAs were generated using the kit Tetro cDNA Synthesis (Bioline). RT-qPCR analysis was performed in a 7500 Real-Time PCR System (Applied Biosystems) using the SYBR Green Reagent protocol (Applied Biosystems). Oligos were created in Geneious Prime (v 2023.2) using Primer-BLAST (NCBI). The ribosomal protein L11 gene (*RpL11*) was used as reference (housekeeper) for normalizing

the expression levels of the genes of interest. Expression fold-change was calculated using the 2^(−ΔΔCt) method, normalized to the level of expression of control flies reared in control diet (100% Cys). To avoid values between 0 and 1, results were log2 transformed. The list of selected genes for evaluation, primer sequence and Real Time qPCR data is shown in Table S1G.

QUANTIFICATION AND STATISTICAL ANALYSIS

Statistical analysis—Statistical significance, the test used, and the sample number are given in the figures and figure legends.

Egg-to-pupa and egg-to-adult survival are plotted as percentage mean survivorship. Developmental delay was calculated by normalizing the median time from egg-to-pupa or egg-to adult of a given AAD or AAD/+ to that of w^{1118} flies, for each respective diet. Delay in the timing of developmental progression is then plotted as normalized median developmental delay (days). Differences in survival and developmental delay were assessed by two-way ANOVA followed by Sidak's multiple comparisons test ($p < 0.05$), accounting for genotype-diet interactions, comparing mutants versus respective controls for each diet individually, as well as the response of mutants (or controls) to the different diets.

For the targeted multi-nutrient array, the linear mixed model (R package: lme4) was fitted to analyze the effects of diet, genotype, and their interaction on mean *shop* survival proportion (number of *shop* males out of total), with replicates treated as a random effect.

For the diet switch experiment, significant differences in the number of *shop* versus control individuals to survive to adulthood for each day of transfer to 0% cysteine diet was assessed using a Student's unpaired t test ($p < 0.05$).

A Cox Proportional-Hazards model (R packages: survival and survminer) was adopted to analyze the effects of diet, genotype, and their interaction on longevity of *shop* and controls.

The effect of diet on *shop* larval locomotion and *shop* excitatory junction potentials on muscle synapses were assessed using multiple comparisons one-way ANOVA followed by Tukey's HSD ($p < 0.05$); different letters ("A", "B", etc) indicate distinct significance groups.

Differences in expression among genotypes, as measured by Real-Time qPCR, were assessed using the ΔΔCt values and analyzed by multiple comparisons one-way ANOVA followed by Tukey's HSD ($p < 0.05$); different letters ("A", "B", etc) indicate distinct significance groups.

Metabolic profiling data analysis—Acquired LC-MS/MS data was processed in an untargeted fashion using open source software IDEOM, which initially used msConvert (ProteoWizard)[84] to convert raw LC-MS files to mzXML format and XCMS to pick peaks to convert to.peakML files.[83] Mzmatch was subsequently used for sample alignment and filtering.[94] Metabolites were identified based on accurate mass (<2 ppm) and comparison of their retention time against that determined for compounds in the standard library or predicted on the basis of their physiochemical characteristics.[89] Only metabolites that

were identified with a level of confidence equal to or greater than 6 in IDEOM were used for downstream functional and statistical analyses, using MetaboAnalyst 5.0.[95] Global metabolic variations due to genotype and diet were visualized using PCA, to verify the contribution of each metabolite in the variance of each treatment. One-way ANOVA [false discovery rates (FDR) < 0.05] was used to identify significant changes in metabolite levels. A heatmap was created to visualize the 50 topmost affected metabolites (based on fold change).

Supplementary Material

Refer to Web version on PubMed Central for supplementary material.

ACKNOWLEDGMENTS

We thank the Bloomington Drosophila Stock Center and Christian Klämbt for fly stocks, Oliver Anderson and Harshini Thiyagarajah for technical assistance, and the Australian *Drosophila* Biomedical Research Facility (Ozdros) for stock importation, as well as Christen Mirth, Richard Burke, and members of the Johnson and Piper labs for helpful discussions. This work is supported by a National Health and Medical Research Council Ideas grant (APP1182330) to M.D.W.P. and T.K.J. and a National Institutes of Health grant (5U01HG007530–08) to T.K.J. J.L. and S.M. are supported by Australian Government Research Training Program Scholarships. This study used BPA-enabled (Bioplatforms Australia)/NCRIS (National Collaborative Research Infrastructure Strategy)-enabled infrastructure located at the Monash Proteomics and Metabolomics Facility. The research conducted at the Murdoch Children's Research Institute (MCRI) was supported by the Victorian Government's Operational Infrastructure Support Program. The Chair in Genomic Medicine awarded to J.C. is generously supported by The Royal Children's Hospital Foundation. H.J.B. and O.K. are supported by R24 OD031447 from NIH/ORIP. T.K.J. is supported by an Australian Research Council Future Fellowship.

REFERENCES

1. Waters D, Adeloye D, Woolham D, Wastnedge E, Patel S, and Rudan I (2018). Global birth prevalence and mortality from inborn errors of metabolism: A systematic analysis of the evidence. J. Glob. Health 8, 021102. 10.7189/jogh.08.021102. [PubMed: 30479748]
2. Ferreira CR, van Karnebeek CDM, Vockley J, and Blau N (2019). A proposed nosology of inborn errors of metabolism. Genet. Med. 21, 102–106. 10.1038/s41436-018-0022-8. [PubMed: 29884839]
3. Warmerdam HAG, Termeulen-Ferreira EA, Tseng LA, Lee JY, van Eeghen AM, Ferreira CR, and van Karnebeek CDM (2019). A Scoping Review of Inborn Errors of Metabolism Causing Progressive Intellectual and Neurologic Deterioration (PIND). Front. Neurol. 10, 1369. 10.3389/fneur.2019.01369. [PubMed: 32132962]
4. Vernon HJ, and Manoli I (2021). Milestones in treatments for inborn errors of metabolism: Reflections on Where chemistry and medicine meet. Am. J. Med. Genet. 185, 3350–3358. 10.1002/ajmg.a.62385. [PubMed: 34165242]
5. Prasad C, Dalton L, and Levy H (1998). Role of diet therapy in management of hereditary metabolic diseases. Nutr. Res. 18, 391–402. 10.1016/S0271-5317(98)00029-3.
6. Boyer SW, Barclay LJ, and Burrage LC (2015). Inherited Metabolic Disorders: Aspects of Chronic Nutrition Management. Nutr. Clin. Pract. 30, 502–510. 10.1177/0884533615586201. [PubMed: 26079521]
7. Woolf LI, Griffiths R, and Moncrieff A (1955). Treatment of Phenylketonuria with a Diet Low in Phenylalanine. BMJ 1, 57–64. 10.1136/bmj.1.4905.57. [PubMed: 13219342]
8. Chapman KA, Ostrovsky J, Rao M, Dingley SD, Polyak E, Yudkoff M, Xiao R, Bennett MJ, and Falk MJ (2018). Propionyl-CoA carboxylase pcca-1 and pccb-1 gene deletions in Caenorhabditis elegans globally impair mitochondrial energy metabolism. J. Inherit. Metab. Dis. 41, 157–168. 10.1007/s10545-017-0111-x. [PubMed: 29159707]
9. Otto N, Marelja Z, Schoofs A, Kranenburg H, Bittern J, Yildirim K, Berh D, Bethke M, Thomas S, Rode S, et al. (2018). The sulfite oxidase Shopper controls neuronal activity by regulating glutamate

homeostasis in Drosophila ensheathing glia. Nat. Commun. 9, 3514. 10.1038/s41467-018-05645-z. [PubMed: 30158546]

10. Breuer M, and Patten SA (2020). A Great Catch for Investigating Inborn Errors of Metabolism—Insights Obtained from Zebrafish. Biomolecules 10, 1352. 10.3390/biom10091352. [PubMed: 32971894]
11. van Vliet D, van der Goot E, van Ginkel WG, van Faassen HJR, de Blaauw P, Kema IP, Heiner-Fokkema MR, van der Zee EA, and van Spronsen FJ (2022). The increasing importance of LNAA supplementation in phenylketonuria at higher plasma phenylalanine concentrations. Mol. Genet. Metab. 135, 27–34. 10.1016/j.ymgme.2021.11.003. [PubMed: 34974973]
12. dos Reis EA, Rieger E, de Souza SS, Rasia-Filho AA, and Wannmacher CMD (2013). Effects of a co-treatment with pyruvate and creatine on dendritic spines in rat hippocampus and posterodorsal medial amygdala in a phenylketonuria animal model. Metab. Brain Dis. 28, 509–517. 10.1007/s11011-013-9389-z. [PubMed: 23430365]
13. Mele S, Martelli F, Lin J, Kanca O, Christodoulou J, Bellen HJ, Piper MDW, and Johnson TK (2023). Drosophila as a diet discovery tool for treating amino acid disorders. Trends Endocrinol. Metab. 34, 85–105. 10.1016/j.tem.2022.12.004. [PubMed: 36567227]
14. Sonoshita M, and Cagan RL (2017). Modeling Human Cancers in Drosophila. In Current Topics in Developmental Biology (Elsevier Inc.), pp. 287–309. 10.1016/bs.ctdb.2016.07.008.
15. Piper MDW, Blanc E, Leitão-Gonçalves R, Yang M, He X, Linford NJ, Hoddinott MP, Hopfen C, Soultoukis GA, Niemeyer C, et al. (2014). A holidic medium for Drosophila melanogaster. Nat. Methods 11, 100–105. 10.1038/nmeth.2731. [PubMed: 24240321]
16. Tsai H-Y, Wu S-C, Li J-C, Chen Y-M, Chan C-C, and Chen C-H (2020). Loss of the Drosophila branched-chain α-keto acid dehydrogenase complex (BCKDH) results in neuronal dysfunction. Dis. Model. Mech. 13, dmm044750. 10.1242/dmm.044750. [PubMed: 32680850]
17. Zwarts L, Vulsteke V, Buhl E, Hodge JJL, and Callaerts P (2017). SlgA, encoded by the homolog of the human schizophreniaassociated gene PRODH, acts in clock neurons to regulate Drosophila aggression. Dis. Model. Mech. 10, 705–716. 10.1242/dmm.027151. [PubMed: 28331058]
18. He F, and DiMario PJ (2011). Drosophila delta-1-pyrroline-5-carboxylate dehydrogenase (P5CDh) is required for proline breakdown and mitochondrial integrity-Establishing a fly model for human type II hyperprolinemia. Mitochondrion 11, 397–404. 10.1016/j.mito.2010.12.001. [PubMed: 21168532]
19. Venken KJT, Schulze KL, Haelterman NA, Pan H, He Y, EvansHolm M, Carlson JW, Levis RW, Spradling AC, Hoskins RA, and Bellen HJ (2011). MiMIC: A highly versatile transposon insertion resource for engineering Drosophila melanogaster genes. Nat. Methods 8, 737–743. 10.1038/nmeth.1662. [PubMed: 21985007]
20. Diao F, Ironfield H, Luan H, Diao F, Shropshire WC, Ewer J, Marr E, Potter CJ, Landgraf M, and White BH (2015). Plug-and-play genetic access to drosophila cell types using exchangeable exon cassettes. Cell Rep. 10, 1410–1421. 10.1016/j.celrep.2015.01.059. [PubMed: 25732830]
21. Kanca O, Bellen HJ, and Schnorrer F (2017). Gene tagging strategies to assess protein expression, localization, and function in Drosophila. Genetics 207, 389–412. 10.1534/genetics.117.199968. [PubMed: 28978772]
22. Kanca O, Zirin J, Hu Y, Tepe B, Dutta D, Lin W-W, Ma L, Ge M, Zuo Z, Liu L-P, et al. (2022). An expanded toolkit for Drosophila gene tagging using synthesized homology donor constructs for CRISPR-mediated homologous recombination. Elife 11, e76077. 10.7554/eLife.76077. [PubMed: 35723254]
23. de Vries B, Mamsa H, Stam AH, Wan J, Bakker SLM, Vanmolkot KRJ, Haan J, Terwindt GM, Boon EMJ, Howard BD, et al. (2009). Episodic Ataxia Associated With EAAT1 Mutation C186S Affecting Glutamate Reuptake. Arch. Neurol. 66, 97–101. 10.1001/archneurol.2008.535. [PubMed: 19139306]
24. Epi4K Consortium; McMahon JM., Schneider AL., Petrovski S., Allen AS., Carvill GL., Zemel M., Saykally JE., LaCroix AJ., Heinzen EL., et al. (2016). De Novo Mutations in SLC1A2 and CACNA1A Are Important Causes of Epileptic Encephalopathies. Am. J. Hum. Genet. 99, 287–298. 10.1016/j.ajhg.2016.06.003. [PubMed: 27476654]

25. Knerr I, Colombo R, Urquhart J, Morais A, Merinero B, Oyarzabal A, Pérez B, Jones SA, Perveen R, Preece MA, et al. (2019). Expanding the genetic and phenotypic spectrum of branched-chain amino acid transferase 2 deficiency. J. Inherit. Metab. Dis. 42, 809–817. 10.1002/jimd.12135. [PubMed: 31177572]
26. Strauss KA, Carson VJ, Soltys K, Young ME, Bowser LE, Puffenberger EG, Brigatti KW, Williams KB, Robinson DL, Hendrickson C, et al. (2020). Branched-chain a-ketoacid dehydrogenase deficiency (maple syrup urine disease): Treatment, biomarkers, and outcomes. Mol. Genet. Metab. 129, 193–206. 10.1016/j.ymgme.2020.01.006. [PubMed: 31980395]
27. Staretz-Chacham O, Pode-Shakked B, Kristal E, Abraham SY, Porper K, Wormser O, Shelef I, and Anikster Y (2021). The Effects of a Ketogenic Diet on Patients with Dihydrolipoamide Dehydrogenase Deficiency. Nutrients 13, 3523. 10.3390/nu13103523. [PubMed: 34684524]
28. Grünert SC, Stucki M, Morscher RJ, Suormala T, Bürer C, Burda P, Christensen E, Ficicioglu C, Herwig J, Kölker S, et al. (2012). 3-methylcrotonyl-CoA carboxylase deficiency: Clinical, biochemical, enzymatic and molecular studies in 88 individuals. Orphanet J. Rare Dis. 7, 31. 10.1186/1750-1172-7-31. [PubMed: 22642865]
29. Marti-Sanchez L, Baide-Mairena H, Marcé-Grau A, Pons R, Skouma A, López-Laso E, Sigatullina M, Rizzo C, Semeraro M, Martinelli D, et al. (2021). Delineating the neurological phenotype in children with defects in the *ECHS1* or *HIBCH* gene. J. Inherit. Metab. Dis. 44, 401–414. 10.1002/jimd.12288. [PubMed: 32677093]
30. Vockley J, and Ensenauer R (2006). Isovaleric acidemia: New aspects of genetic and phenotypic heterogeneity. Am. J. Med. Genet. C Semin. Med. Genet. 142C, 95–103. 10.1002/ajmg.c.30089. [PubMed: 16602101]
31. Meyer M, Hollenbeck JC, Reunert J, Seelhöfer A, Rust S, Fobker M, Biskup S, Och U, Linden M, Sass JO, and Marquardt T (2021). 3-Hydroxyisobutyrate dehydrogenase (HIBADH) deficiency—A novel disorder of valine metabolism. J. Inherit. Metab. Dis. 44, 1323–1329. 10.1002/jimd.12410. [PubMed: 34176136]
32. Tavasoli AR, Shervin Badv R, Zschocke J, Ashrafi MR, and Rostami P (2017). Early infantile presentation of 3-methylglutaconic aciduria type 1 with a novel mutation in AUH gene: A case report and literature review. Brain Dev. 39, 714–716. 10.1016/j.braindev.2017.04.007. [PubMed: 28438368]
33. Masnada S, Parazzini C, Bini P, Barbarini M, Alberti L, Valente M, Chiapparini L, De Silvestri A, Doneda C, Iascone M, et al. (2020). Phenotypic spectrum of short-chain enoyl-Coa hydratase-1 (ECHS1) deficiency. Eur. J. Paediatr. Neurol. 28, 151–158. 10.1016/j.ejpn.2020.07.007. [PubMed: 32800686]
34. Grünert SC, and Sass JO (2020). 3-hydroxy-3-methylglutaryl-coenzyme A lyase deficiency: One disease - Many faces. Orphanet J. Rare Dis. 15, 48–8. 10.1186/s13023-020-1319-7. [PubMed: 32059735]
35. Ouyang Q, Kavanaugh BC, Joesch-Cohen L, Dubois B, Wu Q, Schmidt M, Baytas O, Pastore SF, Harripaul R, Mishra S, et al. (2019). GPT2 mutations in autosomal recessive developmental disability: extending the clinical phenotype and population prevalence estimates. Hum. Genet. 138, 1183–1200. 10.1007/s00439-019-02057-x. [PubMed: 31471722]
36. Rumping L, Buttner B, Maier O, Rehmann H, Lequin M, Schlump JU, Schmitt B, Schiebergen-Bronkhorst B, Prinsen HCMT, Losa M, et al. (2019). Identification of a Loss-of-Function Mutation in the Context of Glutaminase Deficiency and Neonatal Epileptic Encephalopathy. JAMA Neurol. 76, 342–350. 10.1001/jamaneurol.2018.2941. [PubMed: 30575854]
37. Häberle J, Shahbeck N, Ibrahim K, Hoffmann GF, and Ben-Omran T (2011). Natural course of glutamine synthetase deficiency in a 3 year old patient. Mol. Genet. Metab. 103, 89–91. 10.1016/j.ymgme.2011.02.001. [PubMed: 21353613]
38. Hoover-Fong JE, Shah S, Van Hove JLK, Applegarth D, Toone J, and Hamosh A (2004). Natural history of nonketotic hyperglycinemia in 65 patients. Neurology 63, 1847–1853. 10.1212/01.WNL.0000144270.83080.29. [PubMed: 15557500]
39. Kraoua I, Wiame E, Kraoua L, Nasrallah F, Benrhouma H, Rouissi A, Turki I, Chaabouni H, Briand G, Kaabachi N, et al. (2013). 3-Phosphoglycerate Dehydrogenase Deficiency: Description of Two New Cases in Tunisia and Review of the Literature. Neuropediatrics 44, 281–285. 10.1055/s-0033-1338133. [PubMed: 23564319]

40. García-Cazorla À, Verdura E, Juliá-Palacios N, Anderson EN, Goicoechea L, Planas-Serra L, Tsogtbaatar E, Dsouza NR, Schluter €A., Urreizti R., et al. (2020). Impairment of the mitochondrial one-carbon metabolism enzyme SHMT2 causes a novel brain and heart developmental syndrome. Acta Neuropathol. 140, 971–975. 10.1007/s00401-020-02223-w. [PubMed: 33015733]
41. Bienfait HME, Baas F, Koelman JHTM, de Haan RJ, van Engelen BGM, Gabreë ls-Festen AAWM., Ongerboer de Visser BW., Meggouh F., Weterman MAJ., De Jonghe P., et al. (2007). Phenotype of Charcot-Marie-Tooth disease Type 2. Neurology 68, 1658–1667. 10.1212/01.wnl.0000263479.97552.94. [PubMed: 17502546]
42. Oxenkrug G, van der Hart M, Roeser J, and Summergrad P (2017). Peripheral kynurenine-3-monooxygenase deficiency as a potential risk factor for metabolic syndrome in schizophrenia patients. Integr. Clin. Med. 1, 1–3. 10.15761/ICM.1000105.
43. Bozaci AE, Yazici H, Canda E, Uç ar SK., Guvenc MS., Berdeli A., Habif S., and Coker M. (2022). Long-term follow-up of alkaptonuria patients: single center experience. J. Pediatr. Endocrinol. Metab. 35, 913–923. 10.1515/jpem-2022-0004. [PubMed: 35671204]
44. Najafi R, Mostofizadeh N, and Hashemipour M (2018). A Case of Tyrosinemia Type III with Status Epilepticus and Mental Retardation. Adv. Biomed. Res. 7, 7. 10.4103/2277-9175.223740. [PubMed: 29456978]
45. van Spronsen FJ, Blau N, Harding C, Burlina A, Longo N, and Bosch AM (2021). Nat. Rev. Dis. Primers 7, 36. 10.1038/s41572-021-00267-0. [PubMed: 34017006]
46. Baumgartner MR, Rabier D, Nassogne M-C, Dufier J-L, Padovani J-P, Kamoun P, Valle D, and Saudubray J-M (2005). Δ1-pyrroline-5-carboxylate synthase deficiency: neurodegeneration, cataracts and connective tissue manifestations combined with hyperammonaemia and reduced ornithine, citrulline, arginine and proline. Eur. J. Pediatr. 164, 31–36. 10.1007/s00431-004-1545-3. [PubMed: 15517380]
47. Namavar Y, Duineveld DJ, Both GIA, Fiksinski AM, Vorstman JAS, Verhoeven-Duif NM, and Zinkstok JR (2021). Psychiatric phenotypes associated with hyperprolinemia: A systematic review. Am. J. Med. Genet. B Neuropsychiatr. Genet. 186, 289–317. 10.1002/ajmg.b.32869. [PubMed: 34302426]
48. Guo D.c., Gong L, Regalado ES, Santos-Cortez RL, Zhao R, Cai B, Veeraraghavan S, Prakash SK, Johnson RJ, Muilenburg A, et al. (2015). MAT2A Mutations Predispose Individuals to Thoracic Aortic Aneurysms. Am. J. Hum. Genet. 96, 170–177. 10.1016/j.ajhg.2014.11.015. [PubMed: 25557781]
49. Claerhout H, Witters P, Ré gal L., Jansen K., Van Hoestenberghe MR., Breckpot J., and Vermeersch P. (2018). Isolated sulfite oxidase deficiency. J. Inherit. Metab. Dis. 41, 101–108. 10.1007/s10545-017-0089-4. [PubMed: 28980090]
50. Atwal PS, and Scaglia F (2016). Molybdenum cofactor deficiency. Mol. Genet. Metab. 117, 1–4. 10.1016/j.ymgme.2015.11.010. [PubMed: 26653176]
51. Palmieri F (2014). Mitochondrial transporters of the SLC25 family and associated diseases: a review. J. Inherit. Metab. Dis. 37, 565–575. 10.1007/s10545-014-9708-5. [PubMed: 24797559]
52. Hayasaka K (2021). Metabolic basis and treatment of citrin deficiency. J. Inherit. Metab. Dis. 44, 110–117. 10.1002/jimd.12294. [PubMed: 32740958]
53. Nagamani SCS, Erez A, and Lee B (2012). Argininosuccinate lyase deficiency. Genet. Med. 14, 501–507. 10.1038/gim.2011.1. [PubMed: 22241104]
54. Crombez EA, and Cederbaum SD (2005). Hyperargininemia due to liver arginase deficiency. Mol. Genet. Metab. 84, 243–251. 10.1016/j.ymgme.2004.11.004. [PubMed: 15694174]
55. Hu Y, Flockhart I, Vinayagam A, Bergwitz C, Berger B, Perrimon N, and Mohr SE (2011). An integrative approach to ortholog prediction for disease-focused and other functional studies. BMC Bioinf. 12, 357. 10.1186/1471-2105-12-357.
56. Martelli F, Quig A, Mele S, Lin J, Fulton TL, Wansbrough M, Barlow CK, Schittenhelm RB, Johnson TK, and Piper MDW (2023). A defined diet for pre-adult Drosophila melanogaster. Preprint at bioRxiv. 10.1101/2023.08.28.555220.

57. Claerhout H, Witters P, Ré gal L., Jansen K., Van Hoestenberghe MR., Breckpot., and Vermeersch P. (2013). Metabolic stroke in a late-onset form of isolated sulfite oxidase deficiency. J. Inherit. Metab. Dis. 41, 263–266. 10.1016/j.ymgme.2013.01.011.
58. Grings M, Moura AP, Parmeggiani B, Marcowich GF, Amaral AU, de Souza Wyse AT, Wajner M, and Leipnitz G (2013). Disturbance of brain energy and redox homeostasis provoked by sulfite and thiosulfate: Potential pathomechanisms involved in the neuropathology of sulfite oxidase deficiency. Gene 531, 191–198. 10.1016/j.gene.2013.09.018. [PubMed: 24035933]
59. Grings M, Moura AP, Amaral AU, Parmeggiani B, Gasparotto J, Moreira JCF, Gelain DP, Wyse ATS, Wajner M, and Leipnitz G (2014). Sulfite disrupts brain mitochondrial energy homeostasis and induces mitochondrial permeability transition pore opening via thiol group modification. Biochim. Biophys. Acta 1842, 1413–1422. 10.1016/j.bbadis.2014.04.022.
60. Tan W-H, Eichler FS, Hoda S, Lee MS, Baris H, Hanley CA, Grant PE, Krishnamoorthy KS, and Shih VE (2005). Isolated Sulfite Oxidase Deficiency: A Case Report With a Novel Mutation and Review of the Literature. Pediatrics 116, 757–766. 10.1542/peds.2004-1897. [PubMed: 16140720]
61. Marshall K-A, Reist M, Jenner P, and Halliwell B (1999). The neuronal toxicity of sulfite plus peroxynitrite is enhancede by glutathione depletion: implications for Parkinson's disease. Free Radic. Biol. Med. 27, 515–520. 10.1016/S0891-5849(99)00094-5. [PubMed: 10490270]
62. Johnson JL, and Rajagopalan KV (1982). Structural and metabolic relationship between the molybdenum cofactor and urothione. Proc. Natl. Acad. Sci. 79, 6856–6860. 10.1073/pnas.79.22.6856. [PubMed: 6960353]
63. Kohl JB, Mellis AT, and Schwarz G (2019). Homeostatic impact of sulfite and hydrogen sulfide on cysteine catabolism. Br. J. Pharmacol. 176, 554–570. 10.1111/bph.14464. [PubMed: 30088670]
64. Belaidi AA, Rö per, J., Arjune, S., Krizowski, S., Trifunovic, A., and Schwarz, G. (2015). Oxygen reactivity of mammalian sulfite oxidase provides a concept for the treatment of sulfite oxidase deficiency. Biochem. J. 469, 211–221. 10.1042/BJ20140768. [PubMed: 26171830]
65. Sardiello M, Annunziata I, Roma G, and Ballabio A (2005). Sulfatases and sulfatase modifying factors: an exclusive and promiscuous relationship. Hum. Mol. Genet. 14, 3203–3217. 10.1093/hmg/ddi351. [PubMed: 16174644]
66. Barton LL, Ritz NL, Fauque GD, and Lin HC (2017). Sulfur Cycling and the Intestinal Microbiome. Dig. Dis. Sci. 62, 2241–2257. 10.1007/s10620-017-4689-5. [PubMed: 28766244]
67. Choi BJ, Imlach WL, Jiao W, Wolfram V, Wu Y, Grbic M, Cela C, Baines RA, Nitabach MN, and McCabe BD (2014). Miniature Neurotransmission Regulates Drosophila Synaptic Structural Maturation. Neuron 82, 618–634. 10.1016/j.neuron.2014.03.012. [PubMed: 24811381]
68. Camp KM, Lloyd-Puryear MA, and Huntington KL (2012). Nutritional treatment for inborn errors of metabolism: Indications, regulations, and availability of medical foods and dietary supplements using phenylketonuria as an example. Mol. Genet. Metab. 107, 3–9. 10.1016/j.ymgme.2012.07.005. [PubMed: 22854513]
69. Firman S, Witard OC, O'Keeffe M, and Ramachandran R (2021). Dietary protein and protein substitute requirements in adults with phenylketonuria: A review of the clinical guidelines. Clin. Nutr. 40, 702–709. 10.1016/j.clnu.2020.11.003. [PubMed: 33308842]
70. Bickel H, Gerrard J, and Hickmans EM (1953). Influence of phenylalanine intake on phenylketonuria. Lancet (London, England) 265, 812–813. 10.1016/s0140-6736(53)90473-5. [PubMed: 13098090]
71. Aliu E, Kanungo S, and Arnold GL (2018). Amino acid disorders. Ann. Transl. Med. 6, 471. 10.21037/atm.2018.12.12. [PubMed: 30740402]
72. Touati G, Rusthoven E, Depondt E, Dorche C, Duran M, Heron B, Rabier D, Russo M, and Saudubray JM (2000). Dietary therapy in two patients with a mild form of sulphite oxidase deficiency. Evidence for clinical and biological improvement. J. Inherit. Metab. Dis. 23, 45–53. 10.1023/A:1005646813492. [PubMed: 10682307]
73. Del Rizzo M, Burlina AP, Sass JO, Beermann F, Zanco C, Cazzorla C, Bordugo A, Giordano L, Manara R, and Burlina AB (2013). Metabolic stroke in a late-onset form of isolated sulfite oxidase deficiency. Mol. Genet. Metab. 108, 263–266. 10.1016/j.ymgme.2013.01.011. [PubMed: 23414711]

74. ter Borg S, Luiking YC, van Helvoort A, Boirie Y, Schols JMGA, and de Groot CPGM (2019). Low Levels of Branched Chain Amino Acids, Eicosapentaenoic Acid and Micronutrients are Associated with Low Muscle Mass, Strength and Function in Community-Dwelling Older Adults. J. Nutr. Health Aging 23, 27–34. 10.1007/s12603-018-1108-3. [PubMed: 30569065]

75. Calvani R, Picca A, Marini F, Biancolillo A, Gervasoni J, Persichilli S, Primiano A, Coelho-Junior HJ, Bossola M, Urbani A, et al. (2018). A Distinct Pattern of Circulating Amino Acids Characterizes Older Persons with Physical Frailty and Sarcopenia: Results from the BIOSPHERE Study. Nutrients 10, 1691. 10.3390/nu10111691. [PubMed: 30404172]

76. Mayne ST, Playdon MC, and Rock CL (2016). Diet, nutrition, and cancer: past, present and future. Nat. Rev. Clin. Oncol. 13, 504–515. 10.1038/nrclinonc.2016.24. [PubMed: 26951041]

77. Bianchi VE, Herrera PF, and Laura R (2021). Effect of nutrition on neurodegenerative diseases. A systematic review. Nutr. Neurosci. 24, 810–834. 10.1080/1028415X.2019.1681088. [PubMed: 31684843]

78. Lee P-T, Zirin J, Kanca O, Lin W-W, Schulze KL, Li-Kroeger D, Tao R, Devereaux C, Hu Y, Chung V, et al. (2018). A gene-specific T2A-GAL4 library for Drosophila. Elife 7, e35574. 10.7554/eLife.35574. [PubMed: 29565247]

79. Kanca O, Zirin J, Garcia-Marques J, Knight SM, Yang-Zhou D, Amador G, Chung H, Zuo Z, Ma L, He Y, et al. (2019). An efficient CRISPR-based strategy to insert small and large fragments of DNA using short homology arms. Elife 8, e51539. 10.7554/eLife.51539. [PubMed: 31674908]

80. Nagarkar-jaiswal S, Lee P, Campbell ME, Chen K, Anguiano-zarate S, Gutierrez MC, Busby T, Lin W, He Y, Schulze KL, et al. (2015). A library of MiMICs allows tagging of genes and reversible, spatial and temporal knockdown of proteins in Drosophila, pp. 1–28. 10.7554/eLife.05338.

81. Kondo S, and Ueda R (2013). Highly Improved Gene Targeting by Germline-Specific Cas9 Expression in Drosophila. Genetics 195, 715–721. 10.1534/genetics.113.156737. [PubMed: 24002648]

82. Abreu-Blanco MT, Verboon JM, Liu R, Watts JJ, and Parkhurst SM (2012). Drosophila embryos close epithelial wounds using a combination of cellular protrusions and an actomyosin purse string. J. Cell Sci. 125, 5984–5997. 10.1242/jcs.109066. [PubMed: 23038780]

83. Creek DJ, Jankevics A, Burgess KEV, Breitling R, and Barrett MP (2012). IDEOM: an Excel interface for analysis of LC–MS-based metabolomics data. Bioinformatics 28, 1048–1049. 10.1093/bioinformatics/bts069. [PubMed: 22308147]

84. Chambers MC, Maclean B, Burke R, Amodei D, Ruderman DL, Neumann S, Gatto L, Fischer B, Pratt B, Egertson J, et al. (2012). A cross-platform toolkit for mass spectrometry and proteomics. Nat. Biotechnol. 30, 918–920. 10.1038/nbt.2377. [PubMed: 23051804]

85. Chintapalli VR, Wang J, and Dow JAT (2007). Using FlyAtlas to identify better Drosophila melanogaster models of human disease. Nat. Genet. 39, 715–720. 10.1038/ng2049. [PubMed: 17534367]

86. Krause SA, Overend G, Dow JAT, and Leader DP (2022). FlyAtlas 2 in 2022: enhancements to the Drosophila melanogaster expression atlas. Nucleic Acids Res. 50, D1010–D1015. 10.1093/nar/gkab971. [PubMed: 34718735]

87. Nichols CD, Becnel J, and Pandey UB (2012). Methods to Assay Drosophila Behavior. J. Vis. Exp. 3, 3795. 10.3791/3795.

88. Stoessel D, Nowell CJ, Jones AJ, Ferrins L, Ellis KM, Riley J, Rahmani R, Read KD, McConville MJ, Avery VM, et al. (2016). Metabolomics and lipidomics reveal perturbation of sphingolipid metabolism by a novel anti-trypanosomal 3-(oxazolo[4,5-b]pyridine-2-yl) anilide. Metabolomics 12, 126. 10.1007/s11306-016-1062-1.

89. Creek DJ, Jankevics A, Breitling R, Watson DG, Barrett MP, and Burgess KEV (2011). Toward Global Metabolomics Analysis with Hydrophilic Interaction Liquid Chromatography–Mass Spectrometry: Improved Metabolite Identification by Retention Time Prediction. Anal. Chem. 83, 8703–8710. 10.1021/ac2021823. [PubMed: 21928819]

90. Brooks DS, Vishal K, Kawakami J, Bouyain S, and Geisbrecht ER (2016). Optimization of wrMTrck to monitor Drosophila larval locomotor activity. J. Insect Physiol. 93–94, 11–17. 10.1016/j.jinsphys.2016.07.007.

91. Nussbaum-Krammer CI, Neto MF, Brielmann RM, Pedersen JS, and Morimoto RI (2015). Investigating the Spreading and Toxicity of Prion-like Proteins Using the Metazoan Model Organism C. elegans. J. Vis. Exp, 1–15. 10.3791/52321.

92. Rühl P, and Kletzin A (2017). The Sulfur Oxygenase Reductase Activity Assay: Catalyzing a Reaction with Elemental Sulfur as Substrate at High Temperatures. Bio. Protoc. 7, e2403. 10.21769/BioProtoc.2403.

93. Imlach W, and McCabe BD (2009). Electrophysiological Methods for Recording Synaptic Potentials from the NMJ of Drosophila Larvae. J. Vis. Exp, 1109. 10.3791/1109. [PubMed: 19229189]

94. Scheltema RA, Jankevics A, Jansen RC, Swertz MA, and Breitling R (2011). PeakML/mzMatch: A File Format, Java Library, R Library, and Tool-Chain for Mass Spectrometry Data Analysis. Anal. Chem. 83, 2786–2793. 10.1021/ac2000994. [PubMed: 21401061]

95. Pang Z, Chong J, Zhou G, de Lima Morais DA, Chang L, Barrette M, Gauthier C, Jacques PÉ, Li S, and Xia J (2021). MetaboAnalyst 5.0: narrowing the gap between raw spectra and functional insights. Nucleic Acids Res. 49, W388–W396. 10.1093/nar/gkab382. [PubMed: 34019663]

Highlights

- Many inherited metabolic disorders lack effective treatments
- 35 *Drosophila* models of these disorders are screened for diet interactions
- A nutrigenomic array is applied to flies with isolated sulfite oxidase deficiency
- Cysteine depletion restores physiological and metabolic health in the disease model

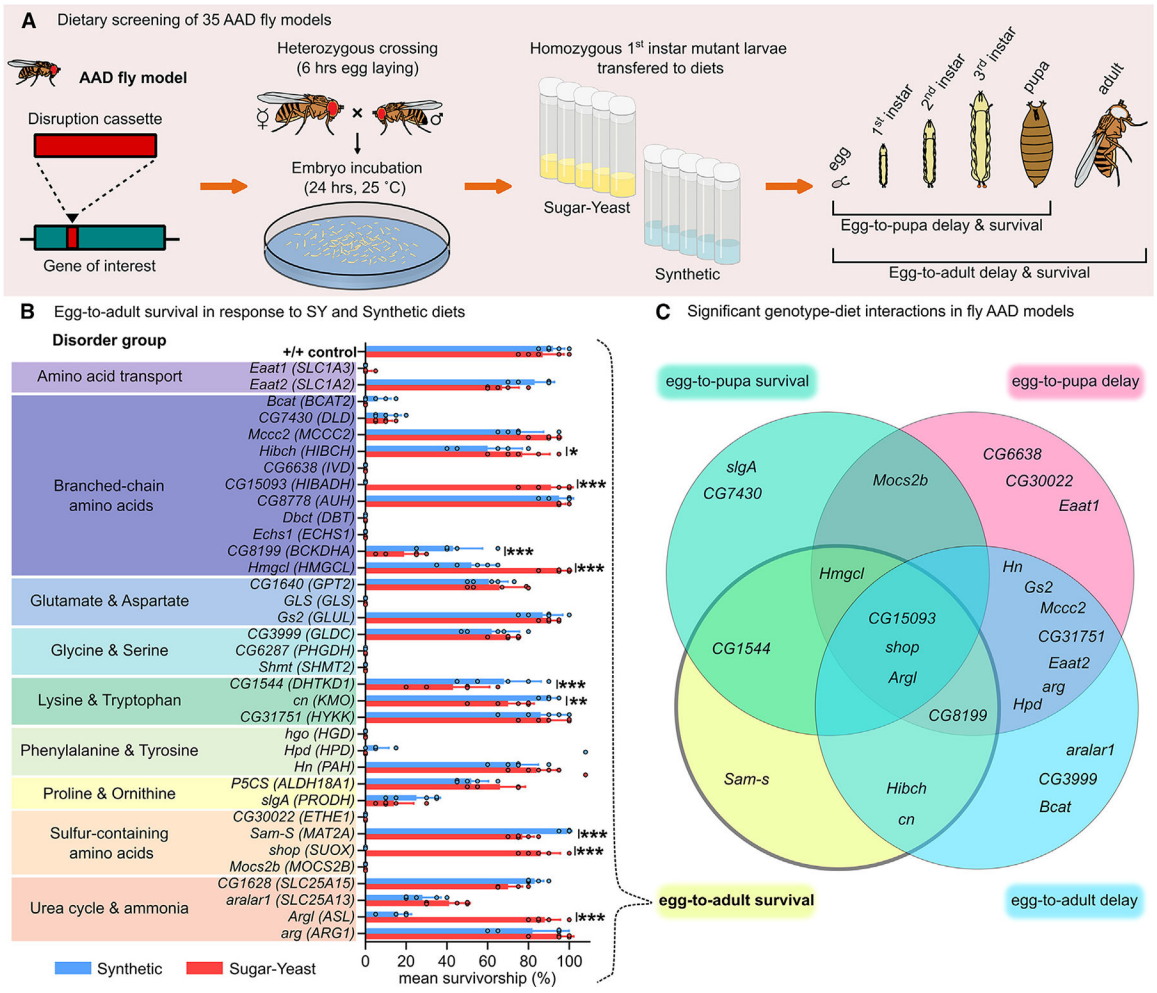

Figure 1. A screen of 35 AAD fly models for phenotypic dietary responses.

(A) The two-diet screen experimental design. Flies heterozygous for loss-of-function alleles (disruption cassette) in human AAD-causing orthologs (red eyed) are mated and homozygous or hemizygous progeny (eventually white eyed) transferred to synthetic or sugar-yeast (SY) media. Time from egg to pupariation and to adult and survivorship were determined. Controls (AAD/+) were obtained by mating heterozygous AAD females and +/+ (w^{1118}) males.

(B) Egg-to-adult survival of fly AAD models in response to SY and synthetic diets. Data points represent the mean ± 1 SD of five replicate vials (dot plots) of 20 individuals per replicate. Two-way ANOVA, Sidak's multiple comparisons test (*adjusted p value [adj p] < 0.05, **adj p < 0.01, and ***adj p < 0.001).

(C) AAD-causing fly orthologs with loss-of-function phenotypes (survival and timing of developmental progression) that change significantly in response to diet (SY and synthetic).

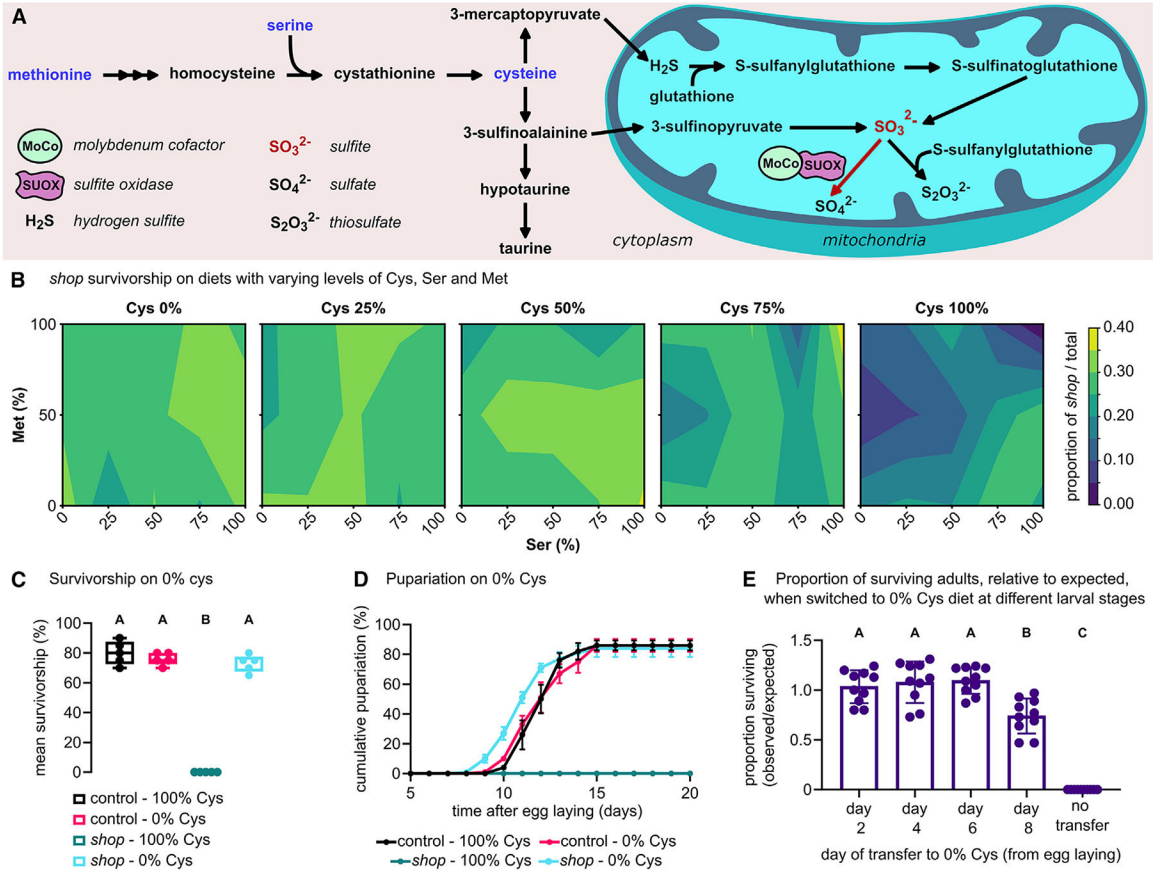

Figure 2. Targeted nutrigenomics to identify diets that redress isolated sulfite oxidase deficiency phenotypes in *Drosophila*.

(A) A simplified schematic of the sulfur-containing amino acid catabolism pathway. Sulfite oxidase (SUOX; encoded by *shop* in Drosophila) catalyzes the conversion of sulfite into sulfate for excretion (red arrow). SUOX, sulfite oxidase; MoCo, molybdenum cofactor; H_2S, hydrogen sulfite; SO_3^{2-}, sulfite; $S_2O_3^{-2}$, thiosulfate; SO_4^{2-}, sulfate.

(B) *shop* survivorship contour plots resulting from a 3-way nutrient (Met, Cys, Ser) dose-response array (75 diets total). Five replicate vials performed per diet (10–80 individuals per replicate).

(C) Percentage egg-to-adult mean survivorship of *shop* and controls reared on complete (100% Cys) or Cys-free (0% Cys) diets. Five replicate vials performed per diet, per genotype, with 20 individuals per replicate. Boxplots show minimum and maximum values, quartile values, and the median.

(D) Pupariation kinetics of *shop* and controls reared on complete (100% Cys) or cysteine-free (0% Cys) diets. Five replicate vials were tested per diet and genotype, with 20 individuals per replicate. Data points with the mean and error bars representing one standard error are shown.

(E) Proportion of surviving *shop* adults, relative to expected Mendelian ratios, when transferred from 100% to 0% Cys diets at days indicated. Bars represent the mean with error bars equal to one standard deviation of 10 replicate vials.

(C and E) Multiple comparisons one-way ANOVA followed by Tukey's honestly significant difference (HSD). Capital letters above columns designate distinct significance groups (groups with the same letter are not significantly different from one another, while groups with different letters are significantly different, $p < 0.001$).

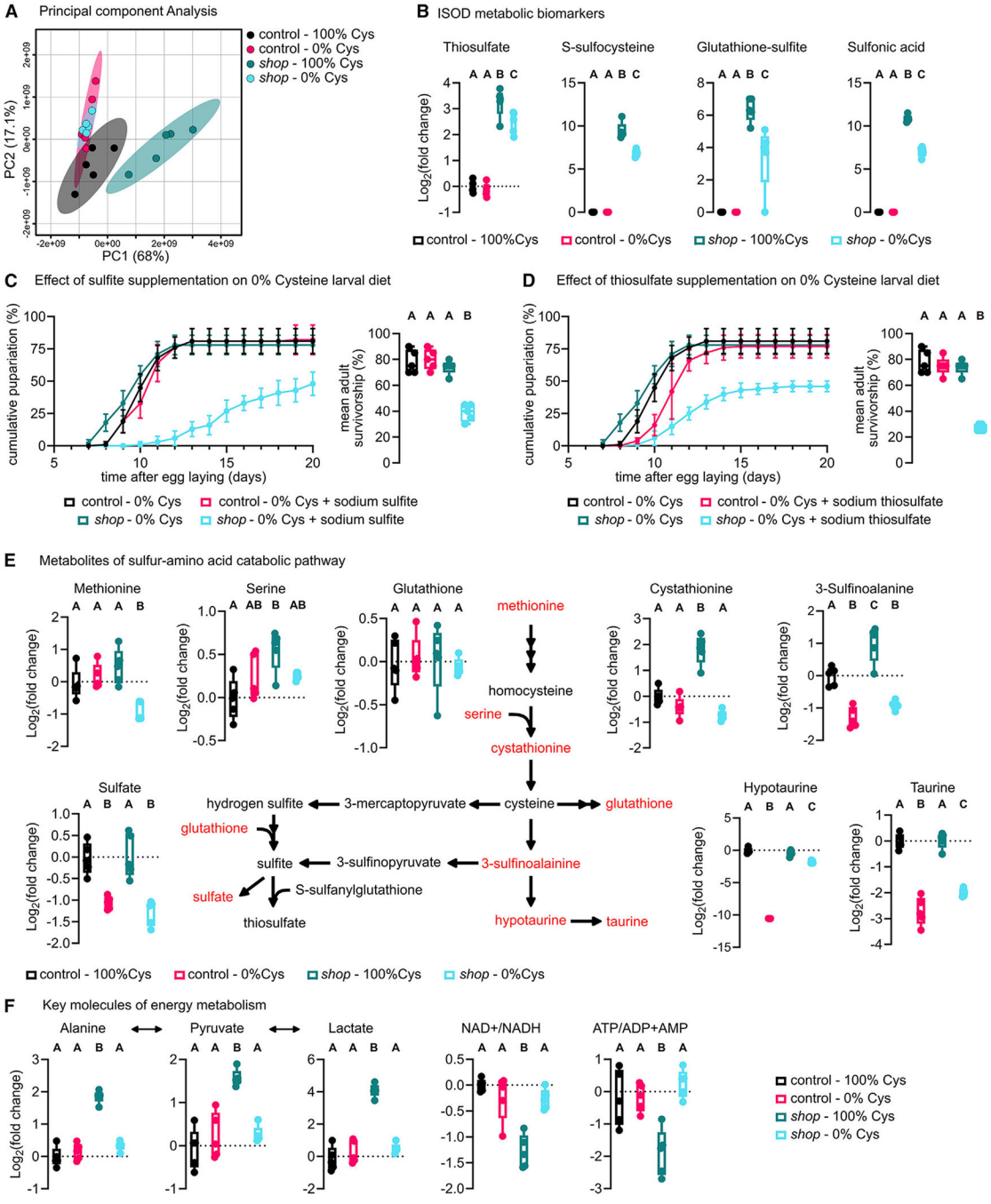

Figure 3. Metabolic profiles of *shop* mutants reared in different diets.

(A) Principal-component analysis (PCA) for metabolite levels in *shop* and control larvae reared on 100% or 0% Cys diet. Each dataset includes five replicates of 25 pooled larvae per replicate.

(B) Levels (log2(fold change) compared to control - 100% Cys) of ISOD-associated metabolites thiosulfate, S-sulfocysteine, and glutathione-sulfite.

(C and D) Cumulative pupariation (%) and egg-to-adult survivorship (%) of *shop* and controls reared on 0% Cys diet supplemented with (C) 2 mM sodium sulfite or (D) 2.5

mM sodium thiosulfate. Data points represent the mean of each time point with error bars equal to one standard error. Five replicate vials were tested per diet and genotype, with 20 individuals per replicate.

(E) Sulfur-amino acid catabolism pathway, metabolite responses to diet in *shop* mutants. Levels (log2(fold change) compared to control - 100% Cys) of sulfur-amino acid catabolism metabolites detected by liquid chromatography-mass spectrometry (LC-MS). *shop* and controls were reared on complete (100% Cys) or cysteine-free (0% Cys) diets. Five replicates were performed per diet and genotype, with 10 individuals per replicate.

(F) Levels (log2(fold change) compared to control - 100% Cys) of energy metabolism metabolites alanine, pyruvate, and lactate and the relative proportions NADH/NAD and ATP/ADP + AMP.

(B, E, and F) Boxplots show minimum and maximum values, quartile values, and the median. Multiple comparison one-way ANOVA with Tukey's HSD. Capital letters above columns designate distinct significance groups (groups with the same letter are not significantly different from one another, while groups with different letters are significantly different, $p < 0.05$).

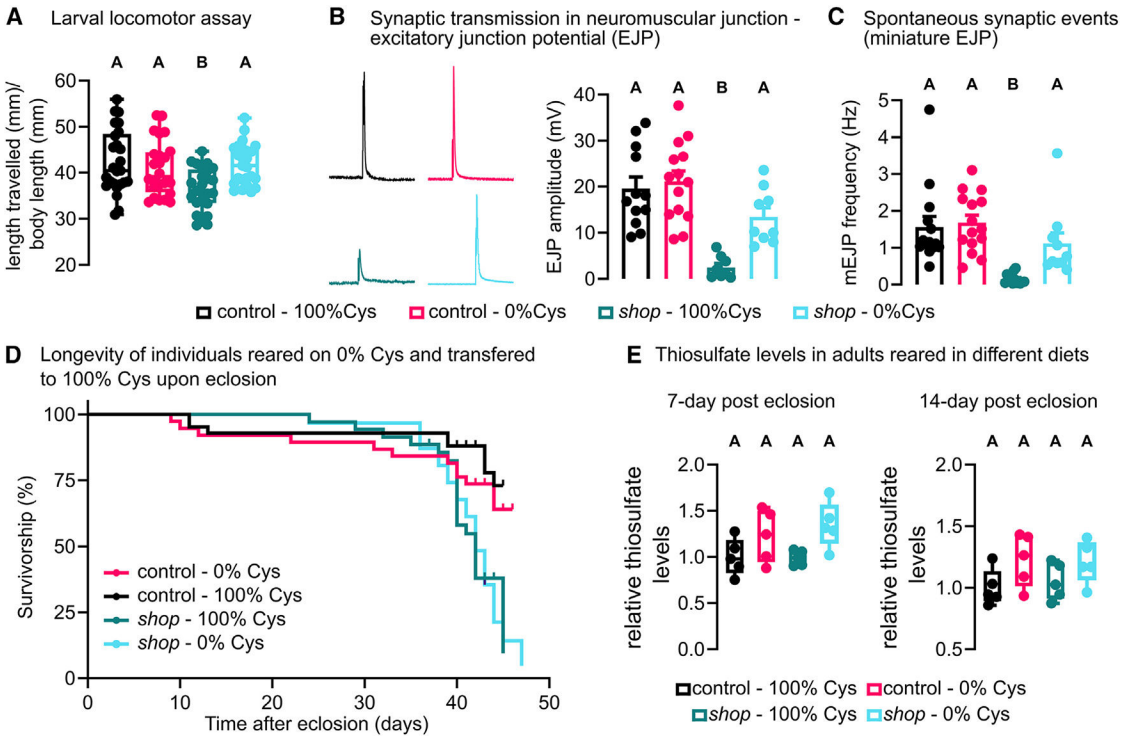

Figure 4. A cysteine-free diet corrects *Drosophila* ISOD metabolic physiology and behavior.

(A) Locomotor behavior assay of 5-day-old *shop* and control larvae reared on 100% or 0% Cys diet. Five replicates were tested per diet and genotype, with 5 individuals per replicate.

(B) Excitatory junction potential (EJP) amplitudes of neuromuscular junctions from second-instar larvae reared on 100% or 0% Cys diet.

(C) Miniature EJP frequency (Hz) measurements from second-instar larvae reared on 100% or 0% Cys diet.

(D) Adult lifespan of *shop* mutants and controls on 100% or 0% Cys diet. Larvae were developed on 0% Cys and, upon adult eclosion, were transferred to 100% Cys diet or remained on 0% Cys diet. There was an effect of genotype ($p < 0.001$, Cox proportional-hazards model) but not of diet ($p = 0.38$, Cox proportional-hazards model) and no evidence for interaction ($p = 0.60$, Cox proportional-hazards model).

(E) Thiosulfate levels of 7-day post-eclosion and 14-day post-eclosion adult *shop* and controls on 100% or 0% Cys diet. Larvae were developed on 0% Cys and, upon adult eclosion, were transferred to 100% Cys diet or kept on 0% Cys diet. Thiosulfate levels were normalized to total protein levels and then made relative to control (100% Cys) samples. Five replicates were performed per diet and genotype, with 10 individuals per replicate.

(A–C and E) Boxplots show minimum and maximum values, quartile values, and the median. Multiple comparison one-way ANOVA followed by Tukey's HSD. Capital letters above columns designate distinct significance groups (groups with the same letter are not significantly different from one another, while groups with different letters are significantly different, $p < 0.05$).

Table 1.

Summary of *Drosophila* AAD models

Human gene	Fly gene[a]	DIOPT orthology score[b]	Disorder name	OMIM[c]	Disease severity	Clinical symptoms
SLC1A3	*Eaat1*	10	glutamate aspartate transporter deficiency	612656	mild	ataxia[23]
SLC1A2	*Eaat2*	12	astroglial glutamate aspartate transporter deficiency	617105	moderate	seizures, delayed psychomotor development, hypotonia[24]
BCAT2	*Bcat*	14	branched-chain aminotransferase 2 deficiency	618850	asymptomatic/mild	developmental delay[25]
BCKDHA	*CG8199*	13	maple syrup urine disease (E1a deficiency)	246900	severe	brain edema, coma, encephalopathy, lethargy, psychomotor delay[26]
DBT	*Dbct*	14	maple syrup urine disease (E2 deficiency)	248600	severe	brain edema, coma, encephalopathy, lethargy, psychomotor delay[26]
DLD	*CG7430*	15	dihydrolipoamide dehydrogenase deficiency/E3 deficiency	246900	severe	hypotonia, liver failure, microcephaly, myopathy[27]
MCCC2	*Mccc2*	14	3-methylcrotonyl-CoA carboxylase 2 deficiency	609014	severe	psychomotor delay, myopathy[28]
HIBCH	*Hibch*	13	3-hydroxyisobutyryl-CoA hydrolase deficiency	610690	severe	psychomotor delay, hypotonia, encephalopathy[29]
IVD	*CG6638*	15	isovaleryl-CoA dehydrogenase deficiency	243500	severe	coma, encephalopathy, feeding difficulties, lethargy[30]
HIBADH	*CG15093*	14	3-hydroxyisobutyrate dehydrogenase deficiency	608475	asymptomatic/mild	psychomotor delay, muscle weakness[31]
AUH	*CG8778*	13	3-methylglutaconyl-CoA hydratase deficiency	600529	moderate	psychomotor delay[32]
ECHS1	*Echs1*	15	mitochondrial short-chain enoyl-CoA hydratase 1 deficiency	616277	severe	psychomotor delay, hypotonia, encephalopathy[33]
HMGCL	*Hmgcl*	14	3-hydroxy-3-methylglutaryl-CoA lyase deficiency	613898	moderate	psychomotor delay, intellectual disability[34]
GPT2	*CG1640*	13	glutamate pyruvate transaminase 2 deficiency	616281	moderate	psychomotor delay, intellectual disability, spastic paraplegia[35]
GLS	*GLS*	14	glutaminase deficiency	618328	severe	seizures, encephalopathy, brain edema[36]
GLUL	*Gs2*	14	glutamine synthetase deficiency	610015	severe	encephalopathy, seizures, hypotonia[37]
GLDC	*CG3999*	14	non-ketoic hyperglycinemia	605899	severe	hypotonia, seizures, intellectual disability, apnea[38]
PHGDH	*CG6287*	14	3-phosphoglycerate dehydrogenase deficiency	601815	severe	microcephaly, epilepsy, seizures, psychomotor delay[39]
SHMT2	*Shmt*	8	mitochondrial serine hydroxymethyltransferase deficiency	619121	severe	developmental delay, intellectual disability[40]
DHTKD1	*CG1544*	15	Charcot-Marie-Tooth disease type 2Q	614984	mild	muscle weakness[41]
KMO	*Cn*	14	kynurenine-3-hydroxylase deficiency	603538	mild	metabolic[42]
HYKK	*CG31751*	13	hydroxylysinuria	236900	mild	intellectual disability

Human gene	Fly gene[a]	DIOPT orthology score[b]	Disorder name	OMIM[c]	Disease severity	Clinical symptoms
HGD	*Hgo*	15	alkaptonuria	203500	mild	arthritis, ochronosis, urine darkening[43]
HPD	*Hpd*	15	4-hydroxyphenylpyruvate dioxygenase deficiency/ tyrosinemia type III	276710	moderate	intellectual disability, seizures[44]
PAH	*hn*	14	phenylketonuria	612349	moderate	intellectual disability, epilepsy[45]
ALDH18A1	*P5CS*	10	δ–1-pyrroline-5-carboxylate synthase deficiency	138250	moderate	psychomotor delay, hypotonia/cutis laxa[46]
PRODH	*SlgA*	15	hyperprolinemia type I	239500	mild	developmental delay, intellectual disability, psychiatric symptoms[47]
ETHE1	*CG30022*	14	mitochondrial sulfur dioxygenase deficiency	602473	severe	psychomotor delay, hypotonia, seizures
MAT2A	*Sam-S*	14	methionine adenosyltransferase II deficiency	601468	mild	thoracic aortic aneurysms[48]
SUOX	*shop*	15	isolated sulfite oxidase deficiency	272300	severe	seizures, encephalopathy, microcephaly[49]
MOCS2B	*Mocs2b*	10	molybdenum cofactor deficiency	603708	severe	encephalopathy, seizures, hypotonia[50]
SLC25A15	*CG1628*	14	mitochondrial ornithine transporter deficiency	603861	moderate	developmental delay, seizures, intellectual disability[51]
SLC25A13	*aralar1*	12	citrin deficiency	603859	moderate	developmental delay, liver dysfunction, psychiatric symptoms[52]
ASL	*Argl*	12	argininosuccinate lyase deficiency	608310	severe	failure to thrive, seizures, coma[53]
ARG1	*arg*	13	arginase deficiency	608313	moderate	seizures, developmental delay, intellectual disability[54]

[a] Gene symbol according to Flybase (http://flybase.org).

[b] DIOPT: score is out of 15. DRSC integrative ortholog prediction tool v.8 (https://www.flymai.org/cgi-bin/DRSC_orthologs.pl).[55]

[c] OMIM: identifier. Online Mendelian Inheritance in Man (https://www.omim.org).

KEY RESOURCES TABLE

REAGENT or RESOURCE	SOURCE	IDENTIFIER
Deposited data		
Metabolomics datasets	MetaboLIGHT	MTBLS9498
Experimental models: Organisms/strains		
w^{1118}	BDSC	RRID:BDSC_3605
shop^{C15}	Otto et al.[9]	
Eaat1$^{CR1303\text{-}TG4.0}$	Lee et al.[78]	RRID:BDSC_86342
Eaat2$^{CR00503\text{-}TG4.2}$	Lee et al.[78]	RRID:BDSC_78932
CG1673$^{CR00316\text{-}TG4.0}$	Lee et al.[78]	RRID:BDSC_79238
CG7430$^{CR00450\text{-}TG4.0}$	Lee et al.[78]	RRID:BDSC_80582
Mccc2$^{CR00361\text{-}TG4.2}$	Lee et al.[78]	RRID:BDSC_79243
CG5044$^{CR70149\text{-}TG4.0}$	Kanca et al.[79]	RRID:BDSC_93364
CG6638$^{CR70183\text{-}KO\text{-}kG4}$	Kanca et al.[80]	RRID:BDSC_94993
CG15093$^{CR70186\text{-}KO\text{-}kG4}$	Kanca et al.[80]	RRID:BDSC_94996
CG8778$^{CR70143\text{-}KO\text{-}kG4}$	Kanca et al.[80]	RRID:BDSC_94981
Dbct$^{CR70199\text{-}TG4.0}$	Kanca et al.[79]	RRID:BDSC_93375
Echs1$^{CR00484\text{-}TG4.1}$	Lee et al.[78]	RRID:BDSC_79270
Hmgcl^{Q25}	This study	
CG8199$^{CR70145\text{-}TG4.2}$	Kanca et al.[79]	RRID:BDSC_92719
CG1640^{CR00025}	Lee et al.[78]	RRID:BDSC_81134
GLS$^{MI09647\text{-}TG4}$	Nagarkar-Jaiswal et al.[81]	RRID:BDSC_53143
Gs2$^{MI14499\text{-}TG4.1}$	Lee et al.[78]	RRID:BDSC_66847
CG3999$^{MI11429C\text{-}TG4.0}$	Lee et al.[78]	RRID:BDSC_66821
CG6287$^{MIC6828\text{-}TG4}$	Nagarkar-Jaiswal et al.[81]	RRID:BDSC_42187
Shmt^{CR0C108}	Lee et al.[78]	RRID:BDSC_81142
CG1544$^{CR00428\text{-}TG4.1}$	Lee et al.[78]	RRID:BDSC_78909
cn$^{CR00701\text{-}TG4.0}$	Lee et al.[78]	RRID:BDSC_80627

Cell Rep. Author manuscript; available in PMC 2024 April 23.

REAGENT or RESOURCE	SOURCE	IDENTIFIER
RStudio	www.rstudio.com	N/A
MetaboAnalyst v5.0	www.metaboanalyst.ca	N/A
Matplotlib v3.7.0	matplotlib.org	N/A
Microsoft Excel	Microsoft 365	N/A
ImageJ	ImageJ.net	N/A
wrMTrck	https://www.phage.dk/plugins/wrmtrck.html	N/A
ffmpeg	https://ffmpeg.org	N/A
Inkscape v1.2.2	https://inkscape.org	N/A
Axograph X v1.7.6	https://axograph.com/	N/A
IDEOM	http://www.creek-lab.com/software85	N/A
msConvert (ProteoWizard)	https://proteowizard.sourceforge.io/index.html86	N/A
Dionex Ultimate 3000 UHPLC	Thermo Scientific	N/A